ChemSusChem

Research Article
doi.org/10.1002/cssc.202301746

Chemistry Europe
European Chemical Societies Publishing

www.chemsuschem.org

VIP *Very Important Paper*

The "*In situ* electrolyte" as a sustainable alternative for the realization of high-power devices

Miriam Sander,[a] Sandesh Darlami Magar,[b] Martin Etter,[c] Andrea Balducci,*[b] and Lars Borchardt*[a]

The "*in situ* electrolyte" displays a concept for electric double-layer- as well as metal-ion capacitors in which the by-products formed during carbon synthesis serve directly as electrolyte salt to minimize waste. In this work, the concept is applied for lithium- and sodium-based systems realizing EDLCs containing aqueous, "Water in Salt" (up to 1.8 V) as well as organic (2.4 V) electrolytes. Via the mechanochemical synthesis, carbon materials with surface areas up to 2000 $m^2 g^{-1}$ and an optimal amount of remaining by-product are designed from the renewable resource lignin. Different cation-anion combinations are enabled by further modification directly inside the pores creating imide-based salts which are tracked by synchrotron *in situ* XRD. By the addition of solvents, the EDLCs show good capacitances up to 21 $F g^{-1}$ combined with excellent rate performances and stabilities. Moreover, the LiTFSI loaded carbon as positive electrode introduces a new tunable lithium alternative for the pre-lithiation of Li-ion capacitors displaying a good rate performance and cyclability.

1. Introduction

In the realm of green chemistry, new device development should prioritize not just performance benchmarks but also the overall environmental footprint, consequently, using renewable feedstock, increasing energy efficiency and preventing waste.[1] The "*in situ* electrolyte" combines all three strategies by utilizing waste products generated during the synthesis of porous carbon materials from renewable sources as a crucial component in the intended application as electric double-layer capacitors (EDLCs). Instead of purifying the final product material and adding an additional electrolyte system, the former waste products are directly used as electrolyte salt (Figure 1a).[2] Thereby, the concept is rooted on two sustainable branches of chemistry. Firstly, EDLCs, which play next to batteries a major role as electrochemical energy storage devices.[3,4] Since their double-layer formation is a purely physical process, EDLCs stand out for an enormous power density (~10 $kW kg^{-1}$) as their charging and discharging takes seconds or less and an exceptional lifetime (> 500,000 cycles).[5] Secondly, the synthesis approach is based on a mechanochemical reaction which is induced and contained via mechanical energy in ball mills without any need of waste producing solvents.[6] Thereby, short reaction times are combined with quantitative yield and no limitation of solubility.[7]

In this work, we showcase the application of the "*in situ* electrolyte" concept to lithium- and sodium-based systems for a variety of aqueous and non-aqueous EDLCs as well as metal-ion capacitors (Figure 1b). The advantages of lithium as the lightest metal with the highest redox potential have long been exploited in the field of energy storage, whereas sodium recently emerged as a suitable alternative due to its greater availability.[8] Porous carbons are an attractive electrode material in commercial applications due to their high specific surface areas (SSA) and good conductivity. A conventional synthesis with relatively low production costs is based on chemical activation at high temperatures of carbonaceous precursors with alkaline or earth alkaline salts, which creates porosity via etching.[9,10,11]

In this work, the condensation reaction between lignin – a renewable waste product from pulp industry – and urea is performed mechanochemically to generate an N-containing precursor (Figure 1b-1) which creates a remarkable N-doped porous carbon with SSA over 2000 $m^2 g^{-1}$.[12] We will display how different activating agents, such as carbonates and hydroxides based on Li and Na, influence the carbon properties. With the conventional use of carbonaceous materials in EDLCs, the pore-blocking waste products from the activation process must be removed by additional purification steps to unlock the full porosity. The resulting waste accumulation, the time consumption and the low mass productivity are the EDLCs main drawbacks for a widespread industrial application. Here instead, the crude composite – porous carbon which pores are

[a] *M. Sander, L. Borchardt*
Inorganic Chemistry I, Ruhr-University Bochum
Universitätstraße 150, 44801 Bochum, Germany
E-mail: lars.borchardt@rub.de

[b] *S. D. Magar, A. Balducci*
Institute for Technical Chemistry and Environmental Chemistry and Center for Energy and Environmental Chemistry Jena (CEEC Jena), Friedrich Schiller University
Philosophenweg 7a, 07743 Jena, Germany
E-mail: andrea.balducci@uni-jena.de

[c] *M. Etter*
Deutsches Elektronen-Synchrotron (DESY)
Notkestraße 85, 22607 Hamburg, Germany

Supporting information for this article is available on the WWW under https://doi.org/10.1002/cssc.202301746

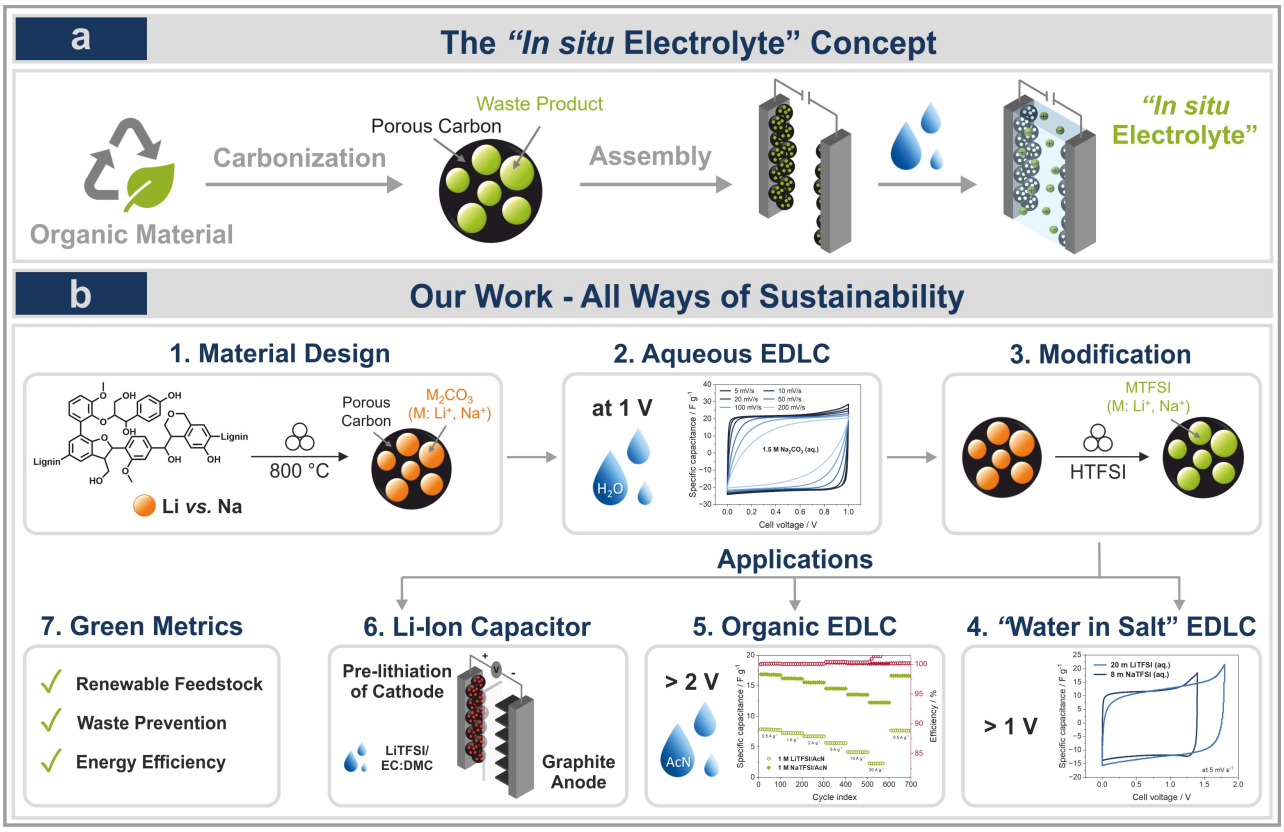

Figure 1. Schematic representation of a) the "*In situ* electrolyte" concept and b) the presented work.

blocked with waste products – can be processed to electrodes by simply adding water, the charging-discharging leads to the *in situ* generated aqueous electrolyte and an operating EDLC (Figure 1b-2).

The main parameters to increase the stored energy in an EDLC are, firstly, the applicable voltage limited by the (electro)chemical stability of the electrolyte and, secondly, the electrode capacitance, which depends on material properties. Regarding electrolyte, aqueous and organic-based EDLCs are the most studied and commercially available system in recent years. The use of aqueous electrolytes allows the realization of non-toxic, high-power devices, which are, however, limited in their generated energy due to the low operative voltage (around 1 V). The use of organic electrolytes, on the other hand, enables the realization of devices with a significantly higher energy density due to an operative voltage up to 3 V.[4,13] However, as common activating agents ($ZnCl_2$,[11] KOH,[14] K_2CO_3,[10] NaCl/KCl[15]) and accordingly the derived by-products are only water-soluble, the resulting EDLCs are limited in their specific energies. To broaden the variety of applications, here the by-product (e.g. alkali carbonate) is directly transformed inside the pores via a mechanochemical solid-state reaction with bis(trifluoromethanesulfonyl) imide acid (HTFSI), whereby non-harmful H_2O and CO_2 evaporate (Figure 1b-3).[16] We successfully demonstrate its application as electrode material in a "Water in Salt" EDLC and organic EDLC to increase the operative voltage window (Figure 1b-4 and 5). Moreover, we display that the *in situ* realized composite electrode when coupled with graphite can be successfully utilized for the realization of lithium-ion capacitors without a need of an external lithium source (Figure 1b-6).

2. Results and Discussion

2.1. Material design

The synthesis of lignin-derived activated carbons by ball milling was adapted from literature and was transferred to an activation procedure with lithium and sodium salts as activating agent.[12] For the standard conditions, the solid reactants lignin, urea and the Li- or Na-based salts (weight ratio 1 : 1 : 1) are used to generate the polymer precursor with incorporated activating agent. The reactants are polymerized for 30 min in a ball mill which is followed by a carbonization at 800 °C (Figure 1b). For activation, the salts lithium carbonate (Li–C), sodium carbonate (Na–C), lithium hydroxide (Li–OH) and sodium hydroxide (Na–OH) are tested. Note, for the hydroxides the molar mass was calculated based on the amount of carbonate and doubled to induce the same amount of alkali metal and to set comparable conditions (Table S1, Supporting Information). The aim of the following part is to create the optimal properties of the composite used for the *in situ* generation of the EDLC electrolyte. This is in particular challenging as the highest

possible amounts of metal salts should remain inside the carbon pores to provide highly concentrated electrolytes in the final application. To showcase the obstacles in more detail: Low amounts of activating agents will yield a carbon of low porosity and likewise provide only little amounts of electrolyte salts. Too high amounts of activating agents, however, bears the danger of destroying the porous carbon structure during a heavy activation step. At the same time the carbon yield will be rather low making this process unprofitable. Varying weight ratios of the activating agents to the C-sources (lignin:urea:agent) are tested in the following.

The polymer (Polym) characterization via infrared (IR) spectroscopy (Figure S1, Supporting Information) showcases the increase in intensity of the bands at 1150 and 1600 cm^{-1} due to the conversion of NH_2 to NH bonds by polycondensation. The activating agents does not participate in the mechanochemical reaction and remains unaltered for all materials, despite using NaOH where unassignable signals appear, most likely caused by the depolymerization of lignin and the decomposition of urea to ammonia due to the high basicity of the hydroxide. By carbonization of the polymers, the composite material (Comp) – nitrogen-doped carbon with incorporated alkali metal salts – is generated. For all used activating agents, the derived by-products verified by powder X-ray diffraction (PXRD) are the corresponding carbonates (Figure S2, Supporting Information) which can be assigned to the activation mechanism by McKee (see Supporting Information).[17] To obtain the pure carbon (Carb) for investigation of its structural properties, the composites are purified. Note, that this additional step is required for the carbon characterization, however, mandatory to omit for the "*in situ* electrolyte" generation.

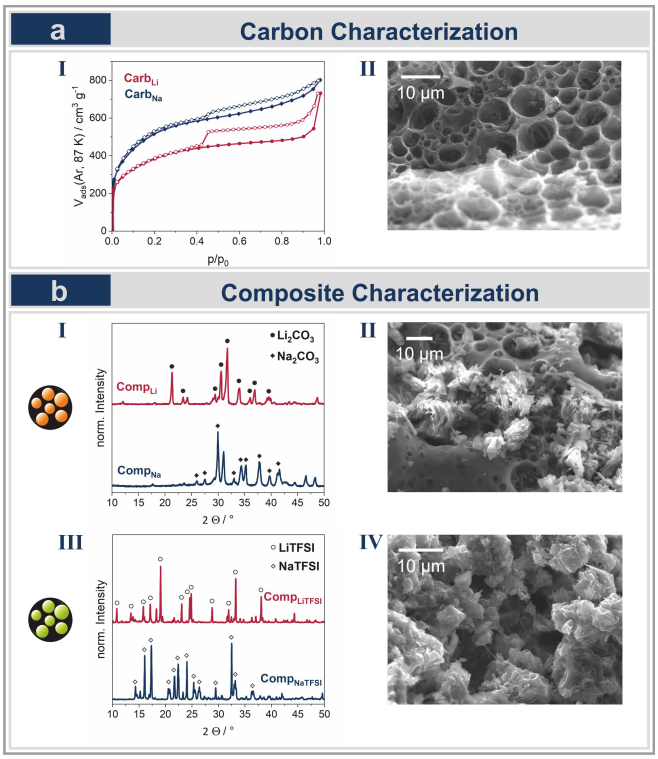

Figure 2. a) I. Argon adsorption/desorption (filled symbols/empty symbols) isotherms recorded at 87 K for the carbons $Carb_{Li}$ and $Carb_{Na}$; II. SEM image of $Carb_{Na}$. b) I. PXRD diffractograms ($\lambda = 1.5406$ Å) of the composites $Comp_{Li}$ and $Comp_{Na}$ with the assigned references (Figure S20, Supporting Information); II. SEM image of $Comp_{Na}$; III. PXRD diffractograms of the modified composites $Comp_{LiTFSI}$ and $Comp_{NaTFSI}$ with the assigned references (Figure S20, Supporting Information); IV. SEM image of $Comp_{NaTFSI}$.

To specify their textural properties the carbons prepared under standard conditions ($Carb_{Li} = Li_2CO_3$; 1:1:1 and $Carb_{Na} = Na_2CO_3$; 1:1:1) are characterized via argon and nitrogen physisorption measurements (see Supporting Information). $Carb_{Li}$ exhibited an SSA of 1223 $m^2 g^{-1}$ (Ar, Table S6, entry 1, Supporting Information) and 1307 $m^2 g^{-1}$ (N_2, Table S7, entry 1, Supporting Information), respectively, whereas for $Carb_{Na}$ we achieved an increased porosity of 1653 $m^2 g^{-1}$ (Ar, Table S6, entry 2, Supporting Information) and 1994 $m^2 g^{-1}$ (N_2, Table S7, entry 7, Supporting Information), respectively. Both carbons create a type IV isotherm (Figure 2a) caused by wide micropores and small mesopores. The hierarchical materials show maximum microporosity at 1.4 nm ($Carb_{Li}$) and 1.7 nm ($Carb_{Na}$), respectively, and mesopores around 2.5 nm (Figure S4a, Supporting Information). Thus, leading to pore volumes V of 0.93 $cm^3 g^{-1}$ ($Carb_{Li}$, Table S6, entry 1, Supporting Information) and 1.02 $cm^3 g^{-1}$ ($Carb_{Na}$, Table S6, entry 2, Supporting Information), respectively. The similarity of the pore structure of the materials despite different activating agents can be explained by its activation mechanism (see Supporting Information). By water-vapor adsorption measurements (Figure S4b, Supporting Information), the filling of the micropores of $Carb_{Li}$ and $Carb_{Na}$ occurs at relative pressures around 0.3 p/p_0, followed by a second step at 0.8 p/p_0 which is related to the filling of the mesopores.[18] The adsorbed V(H_2O) shows values of 0.18 $cm^3 g^{-1}$ and 0.36 $cm^3 g^{-1}$ (Table S6, Supporting Information).[12] According to XPS data, the N-content of both porous carbons totals around 3 wt% (Table S7, Supporting Information). Noteworthy, due to the low N-doping, the data collected via Ar versus N_2 physisorption are comparable (Table S6, entry 1 and 2; Table S7, entry 1 and 7, Supporting Information). Consequently, N_2 was used as adsorptive in the following. To investigate the influence of the mechanochemical treatment the three components lignin, urea and activating agent are carbonized without previous ball milling. The purified carbons (Table S7, entry 19 and 20) showed only a yield of 1% as well as a tremendous decrease of the SSAs. Thus, the pore size distribution shows a shift to larger pores up to 5 nm, whereas the N-content is reduced (< 3 wt%). Consequently, the mechanochemical treatment is pivotal leading to the desired formation of the N-containing polymer precursor and the homogeneous distribution of activating agent therein.

To enable a high salt loading in the composite for a highly concentrated electrolyte, the amount of activating agent was increased up to two times while keeping the lignin and urea content constant. The challenge thereby is to maintain a high SSA with defined pore structure. By increasing the content of lithium carbonate (Table S7, entry 1–3, Supporting Information), we received a less porous material, as demonstrated by the decreased SSA (431 $m^2 g^{-1}$) and V (0.36 $cm^3 g^{-1}$). The yield of

carbon dropped, and the C/N ratio decreased from 25.4 to 12.3. These trends are related to the intensified chemical activation, leading to an increased carbon consumption and its destruction. With sodium carbonate (Table S7, entry 7–9, Supporting Information), on the opposite, the SSA was not affected with around 2000 $m^2 g^{-1}$, whereas its average pore size slightly increased (see Supporting Information). Regarding the alkali hydroxides as activating agents, all materials showed a less defined pore sizes (Figure S9, Supporting Information). Using lithium hydroxide (Table S7, entry 4–6, Supporting Information), the porous carbon showed a similar SSA (around 1000 $m^2 g^{-1}$) like the corresponding carbonate activated and kept a constant value even with increasing amount. Interestingly, the pore sizes became more defined, and the C/N-ratio decreased. In contrast, the sodium hydroxide activated materials (Table S7, entry 10–12, Supporting Information) displayed a constant but lower SSA compared to the corresponding carbonate activated carbons. The V reached high values ($>1.5\ cm^3 g^{-1}$) which, however, cannot make up for the disadvantage of the large and ill-defined pores. Sodium hydroxide is not suitable as the mechanochemical reaction is influenced, consequently, carbon destruction occurs during the chemical activation (see Supporting Information). Overall, the carbons Carb-Li-C-1 ($Carb_{Li}$), Carb-Na-C-1 ($Carb_{Na}$) as well as Carb-Li-OH-2 and Carb-Na-C-2 turned out to be the most promising for the "*in situ* electrolyte" generation. By Inductively coupled plasma atomic emission spectroscopy (ICP-OES) measurements the salt content (M_2CO_3) of the composites was identified (Table S8, Supporting Information). For Comp-Li-C-1 ($Comp_{Li}$) the carbonate content totals 54.5 ± 8.3 wt% with the remainder being porous carbon. Comp-Na-C-1 ($Comp_{Na}$) consists of 52.0 ± 3.0 wt% carbonate, so that for both materials a salt loading of around 1 g_{salt}/g_{carbon} was created. The adapted composites resulted in an increased salt content of 87.8 wt% (Comp-Li-OH-2) and 61.1 wt% (Comp-Na-C-2), respectively. For further material design see Supporting Information.

2.2 Aqueous EDLC

For the electrochemical application, the $Comp_{Na}$ with nearly 61% salt loadings is further processed into free standing electrode (Experimental, Supporting Information). The *in situ* EDLC is thereafter fabricated using two symmetric $Comp_{Na}$ electrodes and water as solvent. The final concentration of the *in situ* electrolyte is controlled by adjusting the amount of water for wetting the separator between two symmetric electrodes and a salt concentration of 1.5 molarity is adapted (see Supporting Information). Under these conditions, the EDLC application is successfully performed (Figure 3). As shown, the normalized cyclic voltammogram of the EDLC displays the typical rectangular shape of these devices, indicating that no faradaic reaction is taking place during the charge-discharge process. A full cell capacitance of 21 $F g^{-1}$ is obtained at 0.5 $A g^{-1}$ which is retained by more than 80% at 5 $A g^{-1}$. The stability is tested by holding cell potential at 1 V for several hundreds of hours. After 500 hours of float time, the device retains almost all its initial capacitance. However, a similar scenario is not possible for $Comp_{Li}$ because of the extremely low solubility of lithium carbonate in water. This limitation was subsequently overcome by adding diluted sulfuric acid generating *in situ* water-soluble sulfate salts and thus successfully the electrolyte (see Supporting Information).

2.3 Modification – From Aqueous to Organic

The right choice of conductive salt and solvent is extremely important for an effective electrolyte system. In the matter of salt, its solubility and good ionic conductivity are among the foremost requirements for its use in the desired solvents. On that note, the nature of anions plays a key role in determining the aforementioned parameters. Imides-based salts, e.g., based on the anion TFSI (bistrifluoromethanesulfonyl imide) with their bulky and stable anions are some of the widely investigated salt components in metal-ion batteries.[19,20] Despite their inability to form an effective passive layer on the aluminum current collector, leading to high risk of anodic dissolution of aluminum

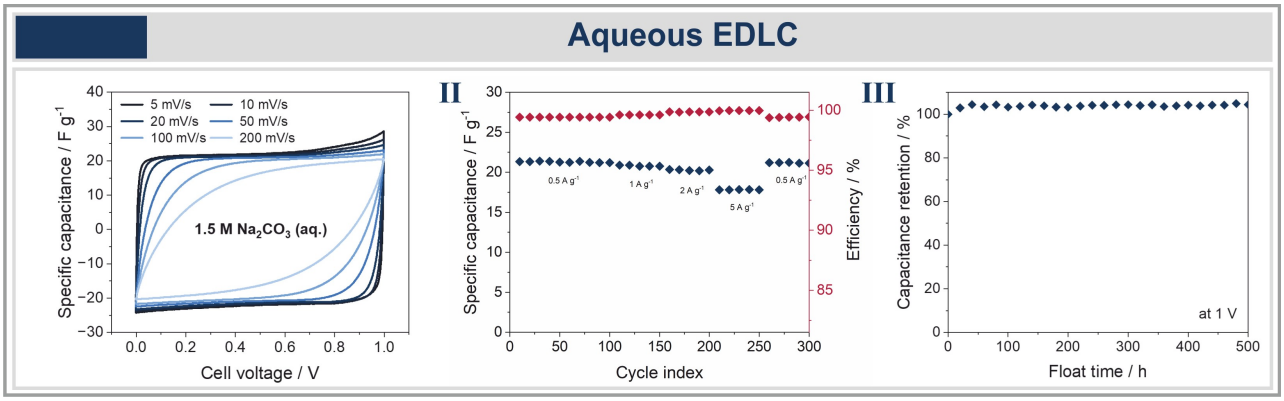

Figure 3. Electrochemical performance of $Comp_{Na}$ based EDLC; I. Normalized cyclic voltammogram; II. Rate performance based on galvanostatic cycling; III. Float test.

at elevated potential, they display high solubility in aqueous[19,21] as well as in many organic solvents.[22] So, correspondingly the first order composites ($Comp_{Li}$, $Comp_{Na}$) are further processed with a motivation to transform the composites from the carbonate salts into bistriflimide salts (LiTFSI and NaTFSI) type, directly inside the pore via a mechanochemical reaction.

To perform a solid-state acid-base reaction, the $Comp_{Li}$ and $Comp_{Na}$ are treated inside the ball mill with the superacid HTFSI to generate the organically soluble LiTFSI and NaTFSI (Figure 1 b). Based on the ICP-OES results, $Comp_{Li}$ and $Comp_{Na}$ are milled for 1 min with the according mass of acid in a molar ratio of 1:2. By this, CO_2 and H_2O are evolving, yielding the pure TFSI salts without the use of additional solvents.[16] Via PXRD pattern (Figure 2b) of $Comp_{Li}$ and $Comp_{Na}$, as well as of the corresponding $Comp_{LiTFSI}$ and $Comp_{NaTFSI}$ the completed mechanochemical modification of alkali metal carbonates to TFSI salts was validated. Additionally, we tracked the mechanochemical salt transformation by synchrotron *in situ* PXRD (Figure 4) whereby $Comp_{Li}$ is treated with HTFSI inside the ball mill. Please note that for this analysis other milling conditions must be chosen (Experimental, Supporting Information), so that, e.g., the milling time cannot be compared to the standard conditions. It is noticeable that the main reflexes of LiTFSI at 13.6°, 15.9°, 18.6°, 18.9° and 32.0° appear, whereas the main reflexes of Li_2CO_3 decrease in intensity. Moreover, energy-dispersive X-ray spectroscopy (EDX) measurements (Figure S21 and S22, Supporting Information) of the initial as well as of the modified composites confirmed the salts and their conversion. By scanning electrode microscopy (SEM) images, an insight how the salt behaves inside the pores can be obtained (Figure 2b, Figure S23, Supporting Information). $Comp_{Li}$ and $Comp_{Na}$ reveal a porous carbon structure which is infiltrated with salt crystals. In contrast, after the modification step the entire carbon surface of $Comp_{LiTFSI}$ and $Comp_{NaTFSI}$ is layered with the organic salts. It is crucial that this interface is made accessible in the EDLC application to reveal its porosity as the composite material indicates only insufficient accessibility of the pores apparent from the low SSAs (Table S7, entry 17 and 18, Supporting Information).

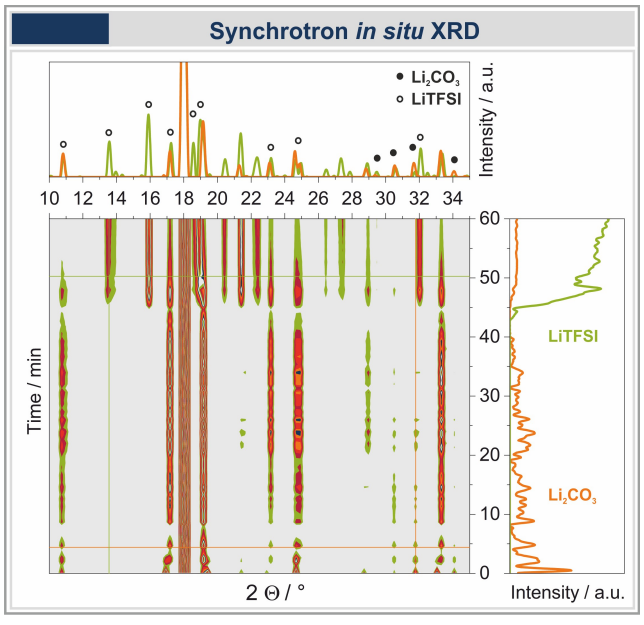

Figure 4. *In situ* X-ray measurement of the mechanochemical reaction from $Comp_{Li}$ with bis(trifluoromethanesulfonyl) imide acid at a milling frequency of 30 Hz. Presented is the 2D plot based the X-ray pattern (λ = 0.20735 Å) converted to Cu Kα1 and the signal intensity over time. The Li_2CO_3 (orange) as well as the LiTFSI (green) can be assigned. Note, at 18° the reflex is assigned to PFA vessel (Figure S26, Supporting Information).

Most important during the modification step is to maintain the textural properties of the porous carbon. By treating the purified carbons under the same milling conditions set for the modification, it was showcased that the porosity was not influenced (Figure S24, Supporting Information). In detail, the SSAs remained at the same values ($Carb_{Li}$: 823 $m^2 g^{-1}$, $Carb_{Li}$ milled: 971 $m^2 g^{-1}$; $Carb_{Na}$: 1788 $m^2 g^{-1}$, $Carb_{Na}$ milled: 1729 $m^2 g^{-1}$) as well as the average pore sizes ($Carb_{Li}$: 3.6 nm, $Carb_{Li}$ milled: 3.4 nm; $Carb_{Na}$: 4.2 nm; $Carb_{Na}$ milled: 4.3 nm). After the salt transformation, we received new salt contents due to the increased mass of the TFSI anion (Table S8, Supporting Information), whereby a salt content of 90.0 ± 2.8 wt% ($Comp_{LiTFSI}$) and 86.0 ± 1.4 wt% ($Comp_{NaTFSI}$, Table S8, Supporting Information) was reached and used further. This corresponds to a salt loading of $< 10\ g_{salt}/g_{carbon}$ for both materials (see Supporting information). Note, the higher the salt content in the composite, the lower the carbon content in the electrode, which can impair the electrode fabrication process and charge storage.

2.4 "Water in Salt" EDLC containing imide-based salt

Due to the high solubility of TFSI-based salt in water, it is possible to realize a Water in Salt (WiS) electrolyte. In this type of electrolyte, the amount of salt considerably outnumbers the solvent in terms of both weight and volume. Thereby, the electrochemical activity of water is greatly suppressed and the electrochemical stability window of the aqueous electrolyte can be broadened beyond its theoretical ESW of around 1.23 V.[19,21]

The *in situ* WiS electrolyte EDLCs are assembled by coupling two symmetric free-standing electrodes of corresponding composites (Experimental, Supporting Information). After the addition of water at low quantities, a final concentration of approximately 8 m of NaTFSI and 20 m LiTFSI is achieved (see Supporting Information). The cyclic voltammetry of the respective cells can be operated at an extended potential window of 0–1.4 V and 0–1.8 V (Figure 5a). Despite a slight redox peak near upper cutoff voltage, the devices show a good capacitive behavior at low scan rate and maintain the rectangular shape at increasing scan rates. When cycled utilizing a current density of 0.5 $A g^{-1}$, the devices $Comp_{NaTFSI}$ and $Comp_{LiTFSI}$ display a capacitance (referred to the total electrode mass) of 11 $F g^{-1}$ and 9 $F g^{-1}$ (Figure 5 a). The devices show good stability during floating test. The capacitance retention of $Comp_{NaTFSI}$ EDLC is above 90% even after 500 hours of float test, while the capacitance retention is nearly 60% for $Comp_{LiTFSI}$ EDLCs (Figure 5a). Taking into account that the electrodes have not been specifically optimized for water-based electrolytes, these results

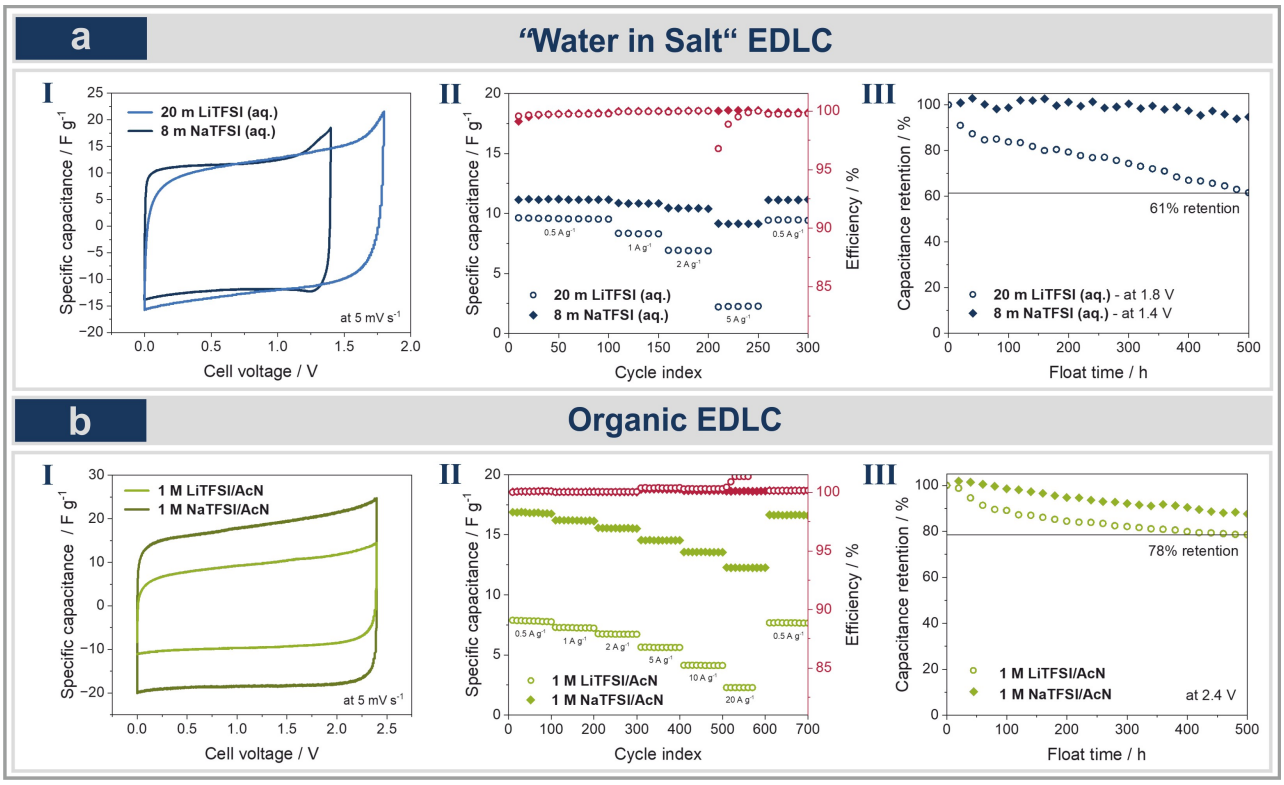

Figure 5. "*In situ* electrolyte" EDLCs containing imide-based salt. a) "Water in Salt" EDLC of $Comp_{LiTFSI}$ and $Comp_{NaTFSI}$ with I. Normalized cyclic voltammogram; II. Rate performance; III. Floating stability. b) Organic EDLC of $Comp_{LiTFSI}$ and $Comp_{NaTFSI}$ with I. Normalized cyclic voltammogram; II. Rate performance; III. Floating stability.

and especially the stability of the $Comp_{NaTFSI}$ based EDLC, are very promising.

2.5 Organic EDLC containing imide-based salt

Thanks to the solubility of the loaded salt, the same electrodes can be further utilized to fabricate organic solvent based EDLCs. With the use of acetonitrile as solvent, the operative potential window of the *in situ* AcN-based EDLC extended up to 2.4 V. A standardized salt concentration of 1 molarity is adapted by adjusting the amount of acetonitrile (see Supporting Information). A typical rectangular shaped cyclic voltammogram with a good capacitance value of 17 $F g^{-1}$ is achieved for EDLC containing $Comp_{NaTFSI}$ which is comparable with that of conventional EDLC, while a total capacitance of 9 $F g^{-1}$ of capacitance is obtained from $Comp_{LiTFSI}$ EDLC (Figure 5b). The rate performance measured at variable current densities shows more than 70% and about 30% of its initial capacitance retention from $Comp_{NaTFSI}$ and $Comp_{LiTFSI}$ at current density of 20 $A g^{-1}$. The device is then further tested for its stability by a constant potential hold at 2.4 V, whereby the device holds more than 70% of its initial capacitance retention after 500 hours (Figure 5b).

Moreover, the respective *ex situ* ELDCs which are conventionally assembled utilizing the purified carbon as electrode and an additional electrolyte are tested under similar protocol. The overall rate performance between the *ex situ* and *in situ* devices is quite comparable (Figure S11 and S28–31, Supporting Information), despite the slightly inferior capacitance values (Figure 6). One of the challenges during wet electrode processing is the hygroscopic nature of LiTFSI salt. As a result, it is difficult to achieve good contact between the electrode slurry and the current collector during casting, which leads to high charge transfer resistance (Figure S28–31, Supporting Information). Similarly, an electrode utilized for WiS electrolyte EDLCs are at double the higher mass loading than its counterpart washed carbon electrode in order to reach high salt concentration in the electrolyte solution (Table S2, Supporting Information). The results reported above are clearly indicating that the *in situ* electrolyte approach can be successfully implemented for the realization of EDLCs containing aqueous (conventional and WiS) as well as organic electrolytes by having different types of cation-anion combinations.

2.6 Application in Lithium-ion capacitor

Metal-ion capacitors are high-power devices comprising a combination of carbonaceous anode such as graphite and hard carbon and an activated carbon (AC) which is used as positive electrode. This electrode combination allows the realization of high voltage devices (4 V), which can display energy and power in between those of EDLCs and metal-ion batteries.[23] The

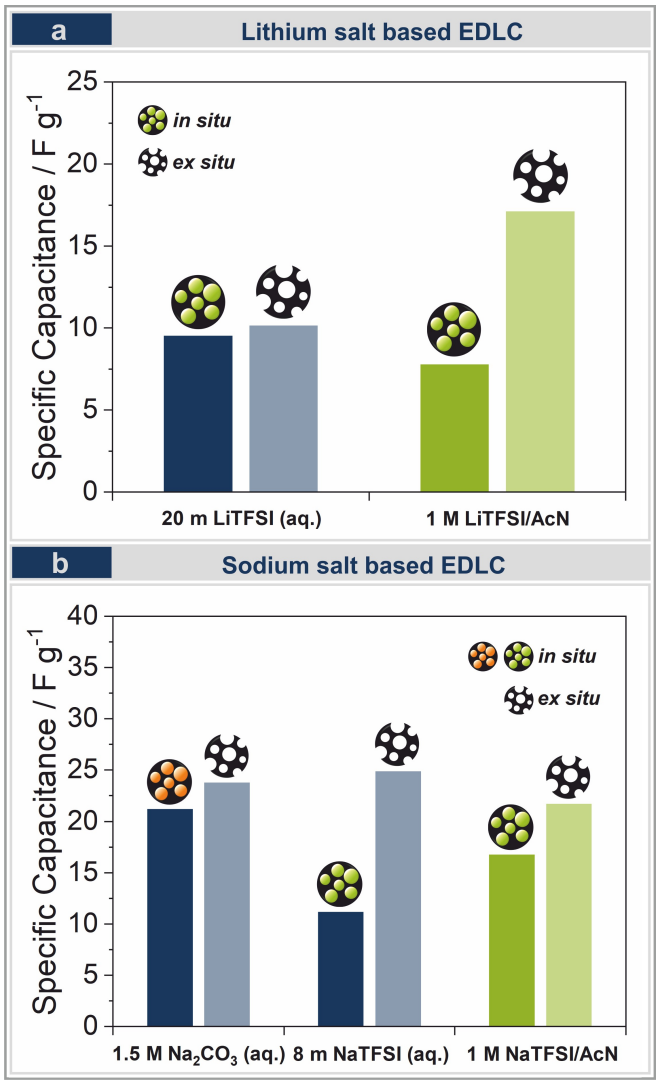

Figure 6. Comparison of the "*in situ* electrolyte" EDLC of Li- and Na-based system with the *ex situ* EDLC (carbon conventionally purified) via the capacitance obtained from galvanostatic cycling at 0.5 A g^{-1}.

interest in MICs increased significantly in the last years and Lithium-ion capacitors (LICs) are nowadays commercially available. One of the challenges associated to the development of LICs is the realization of an effective and safe pre-lithiation of the anode. Since there is not an internal source of lithium ions in the device, this process is mandatory to generate a lithium inventory within the system that is high enough to guarantee the formation of a solid electrolyte interphase (SEI) on the anode and, at the same time, do not cause dramatic concentration gradient within the electrolyte solution. So far several pre-lithiation strategies have been proposed, including the use of i) lithium metal,[24] ii) electrolyte with higher salt concentration,[25] and iii) sacrificial compounds (oxides,[26] nitrides,[27] and salts[28]) each with its advantages and drawbacks.[29] Here instead, the combination of AC loaded with a selected lithium salt as in the *in situ* electrolyte approach and a graphite electrode could be utilized to create a LIC having a high (and tunable) lithium inventory directly during the assembly process. The use of these loaded AC electrodes would not lead to the generation of any dead mass (as in the case of sacrificial cathodes) and would not require the use of any metallic lithium for the pre-lithiation process. To verify if this approach is really feasible, we realized a LIC using AC loaded with LiTFSI. Initially, the performance of the $Comp_{LiTFSI}$ in the electrolyte (1 molar LiTFSI dissolved in 1:1 by vol% mixture of ethylene carbonate: dimethyl carbonate) was investigated using a half cell configuration (vs. Li metal) (Figure S32, Supporting Information). Based on these results and considering the capacity of the graphite electrode in the same electrolyte at different current densities, a mass ratio of 2:1 (positive to negative electrode) was selected for LIC fabrication. It was assembled coupling the $Comp_{LiTFSI}$ electrode with a graphite electrode and filling the cell with the electrolytes containing 1 M LiTFSI in EC: DMC. After the assembly, a current density of 50 mA g^{-1} was applied for the first charge process. During the charge process (Figure 7), the potential of the positive electrode increase (leading to the formation of double layer between the positively polarized electrode and the anion of the electrolyte), while that of the graphite electrode decrease. This latter process is associated with the intercalation of lithium ions with the

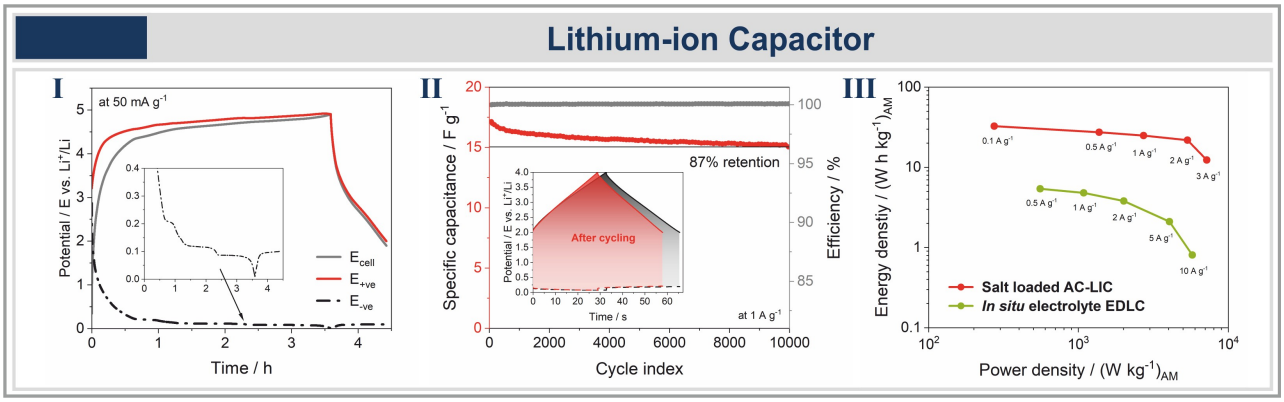

Figure 7. Application of $Comp_{LiTFSI}$ in Li-ion capacitor (salt loaded AC vs. Graphite) with 1 M LiTFSI/EC:DMC; I. Galvanostatic profile of LIC during very first charging step with inset of voltage profile showing graphite intercalation; II. Cycling stability test with inset of the voltage profile before and after cycling; III. Ragone plot of salt-loaded AC-LIC and *in situ* electrolyte EDLC.

graphite electrodes. As shown in the additional figure inset, this process is occurring through subsequent steps, as expected for the graphite electrode. The subsequent cycles were performed between potential window of 2–4 V vs. Li. The device shows a capacitance of 21 $F g^{-1}$ (which is equivalent to capacity of 11 $mA h g^{-1}$) and can be cycled up to current density of 3 $A g^{-1}$ while the capacitance is retained up to 64% (Figure S32, Supporting Information). During long term cycling, it was able to maintain more than 87% of the initial capacitance after 10,000 cycles performed at 1 $A g^{-1}$. Furthermore, it was able to display promising energy and power densities when compared to *in situ* EDLC (Figure 7). It is important to understand that a LIC assembled with conventional empty AC in the same electrolyte (1 M LiTFSI in EC: DMC) against graphite and under similar cycling protocol does not show same level of performance due to an uncompensated irreversible lithium-ion loss. The device lacking lithium source, upon extended cycling, shows a high potential swing with increment in intercalation potential of negative electrode signaling Li-depleted state (Figure S34, Supporting Information). However, using AC loaded with Li salt the device does not experience, on the one hand, a same level of anodic dissolution at first charging step as empty AC (Figure S34, Supporting Information) and, on other hand, the intercalation potential of the negative electrode is much more stable even after 10,000 cycles. To reach a performance level like state-of-the-art LICs, the graphite pre-lithiation protocol, or the fine tuning between carbon porosity and salt loading can be improved. Nonetheless, these results are clearly indicating that preloaded AC electrodes ($Comp_{LiTFSI}$) can be successfully utilized for the realization of LICs, and their advantage for the control of the lithium inventory within the device.

2.7 Green metrics and costs

To showcase the sustainability for the "*in situ* electrolyte" generation, the green metrics mass intensity (MI) as well as mass product (MP) are used. The MP describes how much of the used total mass is preserved in the final product (Eq. 1 and Eq. 2).[30]

$$MI = mass_{total}/mass_{product} \quad (1)$$

$$MP = 1/MI \times 100\,\% \quad (2)$$

We compared the *in situ* electrolyte EDLC with the conventional *ex situ* electrolyte for the standard synthesis of $Comp_{Li}$ and $Comp_{Na}$ (Table S9, Supporting Information). Treating the by-product as waste leads to high MIs which result in low MPs of 5.0% ($Carb_{Li}$) and 8.0% ($Carb_{Na}$). Accordingly, applying the *ex situ* electrolyte only 5% and 8%, respectively, are used of the initial mass of lignin, urea and activating agent for the final material. In contrast, by utilizing the by-product as electrolyte salt the MPs are immensely increased and, indeed, 39% ($Comp_{Li}$) and 33% ($Comp_{Na}$) of the initial mass can directly applied in the final EDLC application using the *in situ* electrolyte EDLC. In addition to these green metrics, however, the various *in situ* systems should be considered more holistically. Therefore, the aqueous-based electrolytes represent the most environment-friendly system due to low toxicity and non-flammability. Another main benefit is the absence of an additional synthesis and preparation of the electrolyte. The simple solid-state salt modification benefits the process safety as the highly skin corrosive TFSI salts must not be handled outside the device in electrolyte solution. Moreover, the reduced cost for the electrolyte synthesis must be considered. The major part of the manufacturing costs of an EDLC can be assigned to the electrode and electrolyte, whereby the conductive salt accounts more than the half of the electrolyte preparation costs.[31] On the one hand, by using the by-product no additional or less costs are necessary as the carbonates can directly be used as conductive salt or are used as one reactant. On the other hand, a comparison of the chemical prices shows that the generation of the alkali metal TFSI salts (LiTFSI, NaTFSI) from carbonates (Li_2CO_3, Na_2CO_3) and HTFSI is for the NaTFSI-system immensely cheaper than the additional purchase of the TFSI salt (Table S10, Supporting Information).

3. Conclusions

In this work, the "*in situ* electrolyte" – a concept in which waste products formed during carbon synthesis are directly used as electrolyte for the final device application – was successfully applied for lithium- and sodium-based systems to realize EDLCs containing aqueous, "Water in Salt" as well as organic electrolytes by having different types of cation-anion combinations. Carbon materials with a high SSA up to 2000 $m^2 g^{-1}$ as well as a high amount of including electrolyte salt were designed mechanochemically using different activating agents. Via solid-state reaction the loaded salt was further converted to create an imide-based electrolyte and a high salt-loading of around 90 wt%. This transformation inside the porous material was tracked by synchrotron *in situ* XRD.

We reported that the salt loaded carbon can be utilized to realize both conventional and "Water in Salt" aqueous electrolyte systems with an increased operative voltage up to 1.8 V in latter case. Thereby, a full cell capacitance of 21 $F g^{-1}$ with high stability during float test was obtained for the Na_2CO_3 containing EDLC. The aqueous NaTFSI (8 m) and LiTFSI (20 m) based EDLCs realized from modified by-product showed 11 $F g^{-1}$ and 9 $F g^{-1}$ at 0.5 $A g^{-1}$, and with less than 10% and 40% capacitance fading after 500 hours of potential hold at upper limit, respectively. When tested with acetonitrile (1 M) at extended operating voltage of 2.4 V, the imide-salt containing materials displayed 17 $F g^{-1}$ (NaTFSI) and 9 $F g^{-1}$ (LiTFSI) with holding more than 70% of initials values after floating. By this, the total material mass preserved in the final product is increased about 30% compared to that of conventional purified carbon based EDLC. Moreover, the TFSI loaded carbon is safely and directly assembled into a lithium-ion capacitor by coupling with graphite as negative electrode. Despite low capacity of 11 $mA h g^{-1}$, it showed good rate performance up to 3 $A g^{-1}$ and

87% retention after 10,000 cycles, introducing a new tunable lithium source for pre-lithiation of metal-ion capacitors.

4. Supporting Information

The authors have cited additional references within the Supporting Information (Ref. [32]).

Acknowledgements

A.B. and S.D.M. would like to thank the financial support from Deutsche Forschungsgemeinschaft (DFG) for projects BA4956/21-1. L.B. and M.S. gratefully acknowledge the Deutsche Forschungsgemeinschaft DFG for the support of the NISECap project (support code: 4538/7-1). We are grateful to DESY (Hamburg, Germany), a member of the Helmholtz Association HGF, for the provision of experimental facilities. Parts of this research were carried out at PETRA III beamline P02.1. Beamtime was allocated by an in-house contingent. An additional thanks to Dr. Wilm Pickhardt and Max Wohlgemuth for the support regarding the *in situ* XRD measurements. We further thank Iris Henkel for all ICP-OES measurements. Open Access funding enabled and organized by Projekt DEAL.

Conflict of Interests

The authors declare no conflict of interest.

Data Availability Statement

The data that support the findings of this study are available from the corresponding author upon reasonable request.

Keywords: in situ electrolyte · pre-lithiation · salt loaded carbon · mechanochemistry · high-power devices

[1] H. C. Erythropel, J. B. Zimmerman, T. M. de Winter, L. Petitjean, F. Melnikov, C. H. Lam, A. W. Lounsbury, K. E. Mellor, N. Z. Janković, Q. Tu et al., *Green Chem.* **2018**, *20*, 1929.
[2] D. Leistenschneider, C. Schneidermann, F. Hippauf, S. Grätz, L. Borchardt, *Adv. Sustainable Syst.* **2018**, *2*, 1800087.
[3] a) P. Simon, Y. Gogotsi, *Nat. Mater.* **2008**, *7*, 845; b) F. Béguin, E. Frąckowiak, *Supercapacitors. Materials, Systems, and Applications*, Wiley-VCH, Weinheim, **2013**, 131; c) J. R. Miller, A. Burke, *Electrochem. Soc. Interface* **2008**, *17*, 53.
[4] F. Béguin, V. Presser, A. Balducci, E. Frackowiak, *Adv. Mater.* **2014**, *26*, 2219–51, 2283.
[5] a) J. Libich, J. Máca, J. Vondrák, O. Čech, M. Sedlaříková, *J. Energy Storage* **2018**, *17*, 224; b) A. G. Pandolfo, A. F. Hollenkamp, *J. Power Sources* **2006**, *157*, 11; c) A. Balducci, *J. Power Sources* **2016**, *326*, 534; d) E. Frackowiak, F. Béguin, *Carbon* **2001**, *39*, 937.
[6] a) F. Gomollón-Bel, *Chem. Int.* **2019**, *41*, 12; b) J.-L. Do, T. Friščić, *Synlett* **2017**, *28*, 2066.
[7] a) A. Stolle, R. Schmidt, K. Jacob, *Faraday Discuss.* **2014**, *170*, 267; b) S. Grätz, D. Beyer, V. Tkachova, S. Hellmann, R. Berger, X. Feng, L. Borchardt, *Chem. Commun.* **2018**, *54*, 5307.
[8] a) M. Li, J. Lu, Z. Chen, K. Amine, *Adv. Mater.* **2018**, *30*, 1800561; b) T. Kim, W. Song, D.-Y. Son, L. K. Ono, Y. Qi, *J. Mater. Chem. A* **2019**, *7*, 2942; c) P. K. Nayak, L. Yang, W. Brehm, P. Adelhelm, *Angew. Chem. Int. Ed.* **2018**, *57*, 102.
[9] a) E. Frackowiak, Q. Abbas, F. Béguin, *J. Energy Chem.* **2013**, *22*, 226; b) T. Surawan, P. S. Priambodo, *2019 16th International Conference on Quality in Research (QIR): International Symposium on Electrical and Computer Engineering, IEEE* **2019**, *1*.
[10] J. Hayashi, A. Kazehaya, K. Muroyama, A. Watkinson, *Carbon* **2000**, *38*, 1873.
[11] Z. Ma, H. Zhang, Z. Yang, Y. Zhang, B. Yu, Z. Liu, *J. Mater. Chem. A* **2014**, *2*, 19324.
[12] C. Schneidermann, N. Jäckel, S. Oswald, L. Giebeler, V. Presser, L. Borchardt, *ChemSusChem* **2017**, *10*, 2416.
[13] C. Zhong, Y. Deng, W. Hu, J. Qiao, L. Zhang, J. Zhang, *Chem. Soc. Rev.* **2015**, *44*, 7484.
[14] M. Evans, E. Halliop, J. MacDonald, *Carbon* **1999**, *37*, 269.
[15] C. Wang, D. Wu, H. Wang, Z. Gao, F. Xu, K. Jiang, *J. Mater. Chem. A* **2018**, *6*, 1244.
[16] D. Leistenschneider, L. H. Heß, A. Balducci, L. Borchardt, *Sustain. Energy Fuels* **2020**, *4*, 2438.
[17] D. W. McKee, *Fuel* **1983**, *62*, 170.
[18] M. Thommes, J. Morell, K. A. Cychosz, M. Fröba, *Langmuir : the ACS journal of surfaces and colloids* **2013**, *29*, 14893.
[19] L. Suo, O. Borodin, T. Gao, M. Olguin, J. Ho, X. Fan, C. Luo, C. Wang, K. Xu, *Science* **2015**, *350*, 938.
[20] a) J. Kalhoff, D. Bresser, M. Bolloli, F. Alloin, J.-Y. Sanchez, S. Passerini, *ChemSusChem* **2014**, *7*, 2939; b) G. Lingua, M. Falco, T. Stettner, C. Gerbaldi, A. Balducci, *J. Power Sources* **2021**, *481*, 228979; c) C. Leibing, D. Leistenschneider, C. Neumann, M. Oschatz, A. Turchanin, A. Balducci, *ChemSusChem* **2023**, *16*, e202300161.
[21] D. Reber, R.-S. Kühnel, C. Battaglia, *Sustain. Energy Fuels* **2017**, *1*, 2155.
[22] a) V. Nilsson, R. Younesi, D. Brandell, K. Edström, P. Johansson, *J. Power Sources* **2018**, *384*, 334; b) N. Xin, Y. Sun, M. He, C. J. Radke, J. M. Prausnitz, *Fluid Phase Equilib.* **2018**, *461*, 1.
[23] a) V. Khomenko, E. Raymundo-Piñero, F. Béguin, *J. Power Sources* **2008**, *177*, 643; b) J. Ajuria, E. Redondo, M. Arnaiz, R. Mysyk, T. Rojo, E. Goikolea, *J. Power Sources* **2017**, *359*, 17; c) S. D. Magar, C. Leibing, J. L. Gómez-Urbano, R. Cid, D. Carriazo, A. Balducci, *Electrochim. Acta* **2023**, *446*, 142104.
[24] a) W. J. Cao, J. F. Luo, J. Yan, X. J. Chen, W. Brandt, M. Warfield, D. Lewis, S. R. Yturriaga, D. G. Moye, J. P. Zheng, *J. Electrochem. Soc.* **2017**, *164*, A93–A98; b) W. J. Cao, J. P. Zheng, *J. Power Sources* **2012**, *213*, 180.
[25] C. Decaux, G. Lota, E. Raymundo-Piñero, E. Frackowiak, F. Béguin, *Electrochim. Acta* **2012**, *86*, 282.
[26] a) M.-S. Park, Y.-G. Lim, J.-H. Kim, Y.-J. Kim, J. Cho, J.-S. Kim, *Adv. Energy Mater.* **2011**, *1*, 1002; b) P. Jeżowski, K. Fic, O. Crosnier, T. Brousse, F. Béguin, *Electrochim. Acta* **2016**, *206*, 440.
[27] Y. Sun, Y. Li, J. Sun, Y. Li, A. Pei, Y. Cui, *Energy Storage Mater.* **2017**, *6*, 119.
[28] a) P. Jeżowski, O. Crosnier, E. Deunf, P. Poizot, F. Béguin, T. Brousse, *Nat. Mater.* **2018**, *17*, 167; b) M. Arnaiz, D. Shanmukaraj, D. Carriazo, D. Bhattacharjya, A. Villaverde, M. Armand, J. Ajuria, *Energy Environ. Sci.* **2020**, *13*, 2441.
[29] a) M. Arnaiz, J. Ajuria, *Batteries & Supercaps* **2021**, *4*, 733; b) L. Jin, C. Shen, A. Shellikeri, Q. Wu, J. Zheng, P. Andrei, J.-G. Zhang, J. P. Zheng, *Energy Environ. Sci.* **2020**, *13*, 2341.
[30] a) K. van Aken, L. Strekowski, L. Patiny, *Beilstein J. Org. Chem.* **2006**, *2*, 3; b) A. D. Curzons, D. N. Mortimer, D. J. C. Constable, V. L. Cunningham, *Green Chem.* **2001**, *3*, 1.
[31] C. Schütter, S. Pohlmann, A. Balducci, *Advanced Energy Materials* **2019**, *9*, 1900334.
[32] D. W. McKee, *Carbon* **1982**, *20*, 59.

Manuscript received: November 24, 2023
Revised manuscript received: January 11, 2024
Accepted manuscript online: January 12, 2024
Version of record online: January 26, 2024